FORMATION OF A PENTAGONAL PARTICLE STRUCTURE FROM COPPER NANOCLUSTERS

A. G. Lipnitskii,[1] D. N. Maradudin,[1] D. N. Klimenko,[1]
E. V. Golosov,[1] I. V. Nelasov,[1] Yu. R. Kolobov,[1] and A. A. Vikarchuk[2]

The structure of pentagonal particles and the processes of their formation from nanoclusters with the fifth-order symmetry axes are investigated by the methods of computer modeling and scanning electron-ion microscopy using copper as an example. It is demonstrated that the mechanism of cluster growth to pentagonal particles can be realized at which the volumetric stress present in noncrystal clusters will be released without breaking of the fifth-order symmetry of the growing cluster shape.

Keywords: nanoclusters, pentagonal particles, copper, modeling.

INTRODUCTION

By the present time, isolated pentagonal particles of the majority of FCC metals have been prepared by various crystallization methods [1]. The particle shapes have the fifth-order axes, and the particle sizes are a few micrometers. For the first time, the researchers succeeded in obtaining the greatest variety of particle types and coatings and films comprising them by the method of electrodeposition of metals from solutions. Despite intensive investigations, the structure of pentagonal particles, mechanism of their growth, and special features of forming their properties caused by the fifth-order symmetry are widely debated topics [1].

In the present work, a mechanism of forming the pentagonal particles from nanoclusters is first investigated by computer modeling on the atomic level. The work is based on the approach described in [2]. The energy of copper nanoclusters shaped as perfect and imperfect decahedrons as well as perfect and imperfect pentagonal nanorods are compared for nanoclusters comprising from 10^3 to 10^6 atoms. As a result of modeling, a mechanism of pentagonal particle growth is suggested that allows volumetric stresses of the nanoclusters to be released retaining the fifth-order symmetry axes of their shapes. Results of modeling are confirmed by investigations of the pentagonal copper rod structure with a Quanta 200 3D scanning electron-ion microscope.

1. GEOMETRY AND CHARACTERISTICS OF THE NANOCLUSTERS

The decahedron cluster structure is described in detail in the literature (for example, see [2] and references therein). Here we briefly describe the characteristics of the atomic cluster structure used below to perform computer modeling of copper clusters and to describe its results.

Figure 1*a* shows a perfect decahedron copper cluster. In this case, the atomic cluster structure is described by the number of atoms *m* on the edge of each tetrahedron and by the number of atoms *N* in the cluster. The decahedron is formed by five tetrahedrons bounded by the {111} crystallographic planes. The tetrahedrons have the edge in common lying on the fifth-order decahedron axis. Each tetrahedron is adjacent to two other tetrahedrons and has the (111) face in common with each neighbor. The remaining tetrahedron faces form the decahedron surface which comprises ten {111}
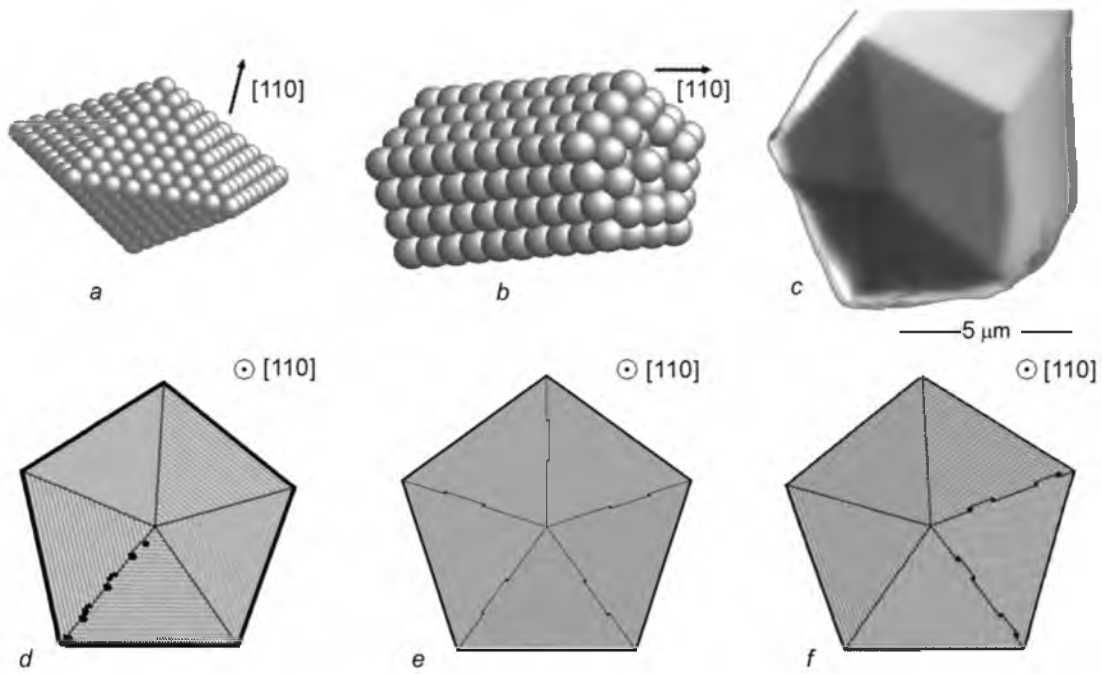
Fig. 1. Perfect decahedron including $N = 609$ copper atoms formed by five deformed tetrahedrons with orientation of the common edge along the [110] crystallographic direction. The edge of each tetrahedron comprises $m = 9$ atoms, the common edge lies on the fifth-order decahedron axis (*a*); perfect nanorod with $l = 10$ and $m = 4$ (*b*); cut of a pentagonal copper rod prepared by electrodeposition (*c*); cross section of the relaxed decahedron cluster comprising $N = 141774$ atoms with built-in close-packed planes (parallel to the [110] direction) near one twin (*d*); cross section of the relaxed decahedron cluster comprising $N = 921503$ atoms with symmetrically built-in close-packed planes of atoms near each twin (*e*); cross section of the nanorod relaxed cluster comprising $N_c = 10289$ columns of atoms with built-in close-packed planes of atoms that fill two gaps between truncated tetrahedrons (*f*).

low-energy faces providing a low surface energy of the decahedron cluster. However, the ideal tetrahedron is enclosed in a solid angle of 70.5° (more precisely, arccos(1/3)); therefore, tetrahedrons must be deformed to fill the decahedron with five tetrahedrons without gaps to compensate for an angle of 7.5° required to obtain 360°. This leads to distortions of the FCC lattice and excessive volume energy, which results in energetically favorable crystal structure without volumetric deformations with increase in the cluster size.

The pentagonal rod (Fig. 1*b*) can be considered as a decahedron in which each tetrahedron is truncated by the (100)-type plane parallel to the fifth-order decahedron axis (for more detailed consideration of the pentagonal nanorod structure, see [3] and the references therein). Taking into account the high ratio of the rod length to its transverse size, we neglect the end faces in calculations of the nanorod energy. This allows periodic boundary conditions to be used along the rod axis. The nanorods are formed by columns of atoms oriented along the rod axis (the [110] close-packed direction). For the examined rod, there are N_c columns comprising l atoms each, so that the number of atoms in the calculation grid is $N = l \times N_c$. For this definition, the quantity l is equal to the period of the calculation grid along the rod axis in units of the shortest spacing of atoms, and N_c is the number of atoms in the plane perpendicular to the rod axis. The cross sectional rod area is proportional to N_c, and the rod radius is proportional to $N_c^{1/2}$.

We note that a continuous decahedron can also be constructed without deformation of tetrahedrons. For this purpose, it is suffice to build additional close-packed planes of atoms in the gaps between tetrahedrons. This will transform the atomic decahedron cluster structure into the crystal structure without excessive volumetric energy with

five intergranular boundaries. As demonstrated the results of this work, exactly the transition to such structures from noncrystal ones with increase in their sizes explains the formation of pentagonal particle structure from growing clusters.

The parameter convenient for a comparison of the stability of clusters having different sizes is given by the expression [2] $\Delta_N = [E_b(N) - N\varepsilon_{coh}]/N^{2/3}$, where ε_{coh} is the cohesive binding energy per atom in the single crystal, $E_b(N)$ is the binding energy of the cluster of N atoms. Thus, Δ_N is the excess cluster energy compared to the perfect single crystal divided by the number of surface atoms proportional to $N^{2/3}$. The excess cluster energy Δ_N can be used to compare directly two clusters of the same sizes based on their excess energies. In addition, the quantity Δ_N is also useful for a comparison of clusters having different sizes and for a description of contributions from the surface, jogs, and volume to the surface cluster energy. Thus, for clusters having the same shapes but different sizes, Δ_N has the form [2]

$$\Delta_N = [cN^{1/3} + bN^{2/3} + aN]/N^{2/3}. \tag{1}$$

Here the parameters c, b, and a describe linear, surface, and volumetric contributions to the surface cluster energy, respectively. The last contribution is present only for clusters with noncrystal structure.

For nanorods, analogous characteristics have the form [3]

$$\Delta_c = [E_b(N) - N\varepsilon_{coh}]/(lN_c^{1/2})$$

and $\hspace{12cm}$ (2)

$$\Delta_c = [c + bN_c^{1/2} + aN_c]/N_c^{1/2}.$$

In this case, Δ_c is the excess nanorod energy compared to the perfect single crystal divided by the number of surface atoms proportional to $lN_c^{1/2}$ for the nanorod.

2. CLUSTER MODELS

Each cluster considered in this work was constructed in two stages. First, the initial arrangement of atoms in the cluster corresponding to a concrete structure type was assigned. Then relaxation to 0 K was carried out by the method of molecular dynamics. The relaxation terminated when the maximal force acting on each atom was <0.5 meV/Å. For nanorods, the period along the rod axis, which decreased under the action of the surface stress, was also relaxed.

In this work, three types of cluster structures in the form of a decahedron and four types of cluster structures in the form of a nanorod were considered. First of all, the noncrystal structure of the perfect decahedron was considered with the above-described initial arrangement of atoms of five deformed tetrahedrons. The initial arrangement of atoms in clusters with the second decahedron structure type comprised five perfect tetrahedrons with additional close-packed planes of atoms filling gaps between two tetrahedrons, as illustrated by Fig. 1d for the cluster from $N = 141774$ atoms. As a result, the cluster was constructed that represented a polycrystal of five grains divided by four perfect twins Σ3(111) and one grain boundary near the twin. Additional planes were built in the clusters if the shortest spacing of atoms did not exceed the radius of the first coordination sphere. Analogously, clusters with other structures illustrated by Fig. 1d, e, and f with reference local structure were constructed. To visualize the atomic cluster structure, we used the definition of the local structure suggested in [4] based on an analysis of the topology of bonds among neighbors of each atom of the object being modeled which was successfully used in [5] to analyze model nanocrystal FCC metal structures. The suggested analysis allows dislocations, twins, stacking faults, grain boundaries, and other defects of the crystal structure as well as regions with reference crystal lattice to be distinguished. With the help of shades of grey color, we distinguished atoms having the local environment of the FCC (light grey color) and HCP lattices (grey color) as well as the local environment other than FCC and HCP lattices (black color).
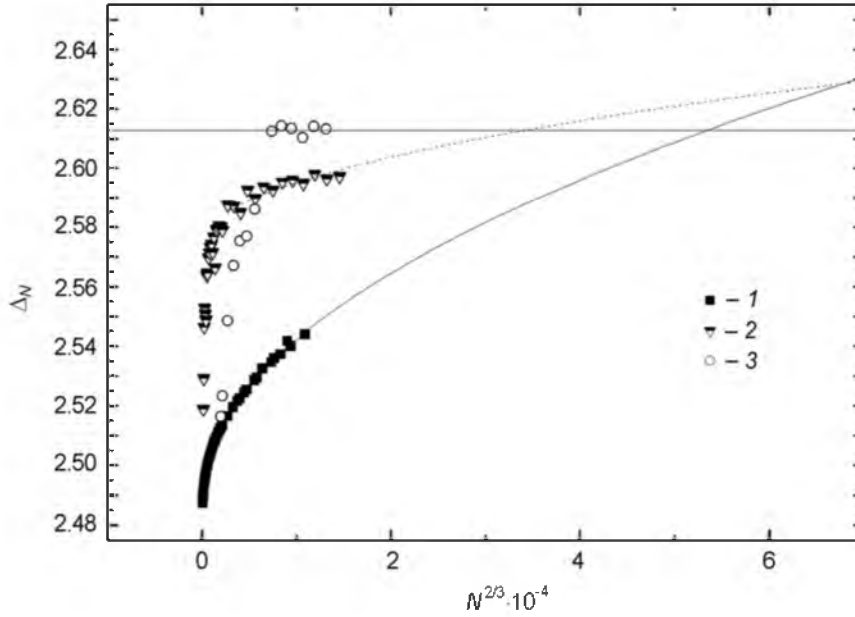
Fig. 2. Calculated energy excess of decahedron copper clusters: Δ_N (in units of electronvolts divided by the number of surface atoms) as a function of $N^{2/3}$. Here *1* denotes the perfect decahedron, *2* is for the imperfect decahedron with one grain boundary deviated from the twin by an angle of 7.5°, and *3* is for the imperfect decahedron with five grain boundaries each deviated from the twin by an angle of 1.5°.

It should be noted that the chosen criterion for the incorporation of additional planes does not provide complete release of the volumetric stress. However, this had no effect on the results of our investigations, and the correction for the residual volume energy was introduced where necessary.

3. RESULTS OF CALCULATIONS AND THEIR DISCUSSION

Figure 2 shows the calculated energy excess Δ_N for decahedron clusters. The interpolation of these values toward larger cluster sizes by Eq. (1) until they intersect the Δ_N plots drawn for perfect and imperfect decahedrons with planes built in one gap between the tetrahedrons is also shown here. From Fig. 2 it can be seen that for clusters with $N^{2/3} = 10,000$ ($N = 1,000,000$), the cluster energies are minimal for the perfect structure, and imperfect decahedrons possess lower energy for the asymmetrical built-in planes (within a solid angle of 7.5°). These energy values demonstrate the determining influence of the surface cluster energy in this interval of cluster sizes. However, an increase in the volume energy with increasing cluster sizes caused by the lattice deformation in the perfect decahedron results in the energetically more favorable formation of the imperfect decahedron in which volumetric deformations decrease due to the built-in planes of atoms. Interpolation shown in Fig. 2 demonstrates that decahedron structures change for clusters formed by 18 million atoms. To estimate the transitive cluster size, we took it equal to the diameter of the sphere whose volume is equal to the total volume of atoms in the cluster. This size is $D_d = 74$ nm. It should be noted that without volumetric stresses, the Δ_N plot for the imperfect decahedrons in Fig. 2 should be saturated at constant $b = 2.613$ calculated by interpolation for increased decahedron sizes, since a significant contribution to the energy excess Δ_N for larger sizes comes only from the surface and internal boundaries. In this regard, we took the corrected value $D_d = 66$ nm ($N = 12.5$ mln atoms) determined as an intersection point of the plot Δ_N for the perfect decahedrons with the straight line $\Delta_N = 2.613$ (Fig. 2).

Figure 3 shows the energy excess Δ_c calculated for the rod clusters. Interpolation of Δ_c with the help of Eq. (2) is also shown in the figure. It started from $N_c^{1/2} = 100$. As can be seen, the growth of the imperfect rods compared to
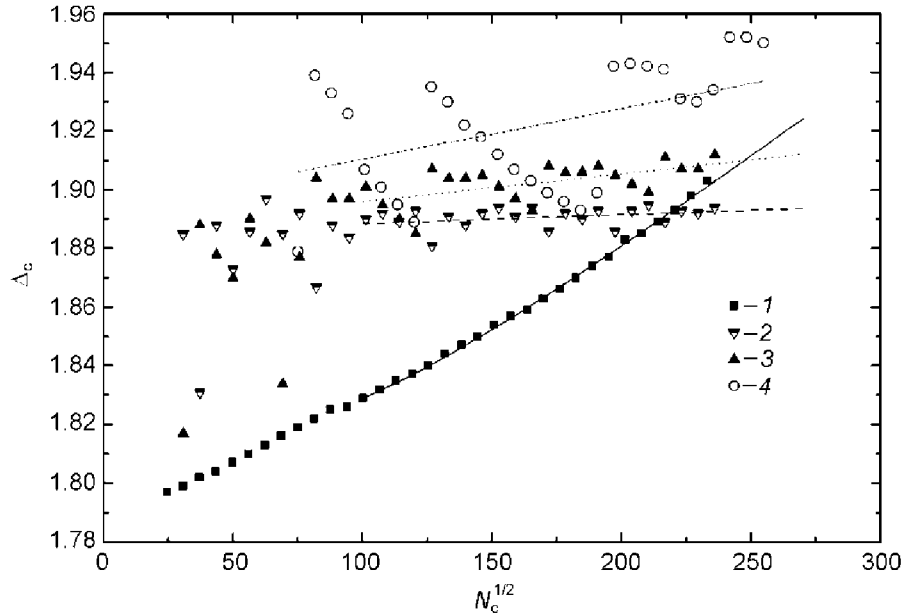
Fig. 3. Calculated energy excess for the pentagonal rod copper clusters: Δ_c (in units of electronvolts divided by the number of surface atoms) as a function of $N_c^{1/2}$. Here *1* denotes the perfect rod, *2* is for the imperfect rod with one grain boundary deviated from the twin by 7.5°, *3* is for the imperfect rod with two grain boundaries each deviated from the twin by an angle of 3.75°, and *4* is for the symmetric imperfect rod with five grain boundaries each deviated from the twin by an angle of 1.5°. The coincidence of the interpolated straight lines with the rod types is seen from the figure.

perfect ones becomes energetically more favorable starting from $N_c^{1/2} = 220$. This corresponds to the pentagonal rod with the (100) face width of 36 nm ($m = 139$) and the diameter of the circle circumscribed about the rod cross section $D_c = 61$ nm. In this case, imperfect pentagonal rods with volumetric stresses released due to asymmetrical incorporation of the additional planes only near one twin Σ3(111) have lower energies.

To analyze the results of modeling, we note that the grain boundaries in the examined imperfect clusters, according to the Brandon criterion [6], belong to special boundaries with inverse density of the coinciding sites Σ = 3, since the deviation from an angle of 70.5° (the perfect twin with Σ = 3) is about $15/(3)^{1/2}$. The fact that the grain boundaries are special causes their special properties, first of all, their low mobility. This was confirmed by experimental investigations of the stability of facets adjacent to the Σ3(111) boundaries in copper with increasing temperature [7]. In [7], the stability of these facets was established for temperatures up to the copper melting temperature.

The results of modeling and the stability of the boundaries with Σ = 3 suggest the following mechanism of pentagonal particle growth from clusters with the fifth-order axes. The structures with the fifth-order axes are formed during cluster growth due to the fact that they are energetically more favorable for small cluster sizes, despite the presence of volumetric deformations. After sizes of about 60 nm, the structures of growing particles change with smooth transition to structures providing volumetric deformation release when particles grow further. The indicated transition in the process of growth is realized because new structures are energetically more favorable and there is no barrier between the initial and subsequent structures. Since the perfect and examined imperfect pentagonal rods grow due to incorporation of additional planes like the (100) ones, there is no barrier when going from the growth of perfect to the subsequent growth of imperfect pentagonal rods. The growth of decahedron clusters has a special feature caused by the dynamic instability of the built-in additional FCC planes, like the (111) ones, on the decahedron surface toward the occurrence of the HCP planes [8]. This causes the cluster shape to change from the decahedron to others. However, as indicated above, in this case the system of grain boundaries close to Σ3(111) is inherited by the growing particle

because of high stability and low mobility of the special grain boundaries with $\Sigma = 3$. In some cases, an icosahedron cluster grows from the decahedron as a result of dynamic instability, since the decahedron is an integral part of the icosahedron [8]. This explains the observed rod and icosahedron shapes of pentagonal particles [1].

To test the asymmetrical character of misorientation of the neighboring crystallites in the pentagonal rods predicted above, the corresponding angles of the copper rod prepared by electrodeposition (whose cut perpendicular to the rod axis is shown in Fig. 1c) were calculated. Calculations of the direct polar figure demonstrated that these angles were (72 ± 0.5), (71 ± 0.5), (71 ± 0.5), (72 ± 0.5), and $(74 \pm 0.5)°$. This does suggest the separation of one boundary with a larger misorientation angle compared to other boundaries.

CONCLUSIONS

As a result of computer modeling of copper clusters, the mechanism of pentagonal particle growth from clusters with the fifth-order axes has been proposed and proved. According to this mechanism, particles having special grain boundaries with inverse density of coinciding sites $\Sigma = 3$ are formed without volumetric deformations.

This mechanism predicts a higher probability of forming pentagonal rods with asymmetrical misorientation of neighboring crystallites forming the rod, in agreement with the experimentally established misorientation angles in the copper rod prepared by electrodeposition.

REFERENCES

1. A. A. Vikarchuk and I. S. Yasnikov, Structurization in Nanoparticles and Microcrystals with Pentagonal Symmetry Formed by Electrocrystallization of Metals [in Russian], Publishing House of Tol'yatti State University, Tol'yatti (2006).
2. F. Baletto and R. Ferrando, Rev. Mod. Phys., 77, No. 1, 371–423 (2005).
3. G. E. Tommei, F. Baletto, R. Ferrando, et al., Phys. Rev., B69, No. 11, 115426–115433 (2004).
4. J. D. Honeycutt and H. C. Andersen, J. Phys. Chem., 91, No. 19, 4950–4963 (1987).
5. H. V. Swygenhoven, Phys. Rev., B62, No. 2, 831–838 (2000).
6. D. G. Brandon, Acta Metal., 14, No. 11, 1479–1484 (1966).
7. B. B. Straumal, S. A. Polyakov, and E. J. Mittemeijer, Acta Mater., 54, 167–172 (2006).
8. F. Baletto, A. Rapallo, G. Rossi, and R. Ferrando, Phys. Rev., B69, No. 23, 235421–235426 (2004).